

## Photo- and Thermodesorption of Helium on Pt(111)

T. Niedermayer,<sup>1</sup> H. Schlichting,<sup>1</sup> D. Menzel,<sup>1</sup> S. H. Payne,<sup>2</sup> and H. J. Kreuzer<sup>2</sup>

<sup>1</sup>*Physik-Department E20, Technische Universität München, D-85747 Garching, Germany*

<sup>2</sup>*Department of Physics, Dalhousie University, Halifax, Nova Scotia, Canada B3H 3J5*

(Received 17 May 2002; published 30 August 2002)

In a detailed study of thermal desorption of monolayers of both  $^4\text{He}$  and  $^3\text{He}$  adsorbed on Pt(111) (binding energy about 9 meV), we have observed photodesorption induced by the blackbody radiation from a room temperature environment. This process proceeds independently of the thermal desorption. Theoretical treatments of both thermal and photodesorption are given and agree very well with the data in all important aspects. We conclude that the photodesorption is due to direct coupling of photons to the adsorbate.

DOI: 10.1103/PhysRevLett.89.126101

PACS numbers: 68.43.Mn, 67.70.+n, 68.43.Tj

Helium, the smallest and simplest closed-shell atom, is a model system for many interactions, including those with each other and on surfaces; it is a prototype for a weakly bound adsorbate. Many theoretical papers on He layers have therefore appeared [1,2] analyzing the properties of the resulting layers, including possible quantum effects. In its main use in surface science, elastic diffraction, and inelastic scattering, helium surface coverage is zero. Owing to its low polarizability, the attractive well in front of a surface is very shallow; this makes experiments on monolayers difficult. Thus, He (sub)monolayers can be prepared only at very low temperatures and, thus far, have been investigated only on high surface area materials such as grafoil [3], and on filaments and films with ill-defined surfaces [4]. Direct desorption experiments have been reported only for the latter; we do not know of any work on well-defined macroscopic single crystal surfaces. A quantum desorption effect has been postulated, in which a single *phonon* knocks a He atom off the surface [5] (see also [1]).

Because of this fundamental importance and the gap between the theoretical and experimental situations, we have studied the adsorption/desorption kinetics of both  $^4\text{He}$  and  $^3\text{He}$  on Pt(111) in detail; here we report the main characteristics. During this work, we also observed photodesorption (PD) induced by the blackbody radiation of a room temperature environment. We demonstrate that this effect is *not* caused by heating the substrate, and *not* by nonequilibrium phonons, but by direct coupling of the incoming photons with the dynamic dipole of the adsorbate (helium atom plus modified surface). Such an effect has been predicted for physisorbed molecules [6] and observed for physisorbed  $\text{H}_2$  and  $\text{D}_2$  on metals [7]. Our theory [8,9] can account for our observations in all important aspects. In particular, the observed PD rate and its dependence on radiation temperature and isotope mass are fully recovered. This proves the observed PD to be a true quantum desorption effect, in which a single *photon* desorbs a He atom.

Experimentally, we had to extend our techniques for cooling well-defined single crystals in surface science

systems (base pressure  $3 \times 10^{-11}$  mbar) [10,11] to sufficiently low temperatures for irreversible adsorption of He monolayers to occur, and to adapt our methods for the measurement of adsorption/desorption rates by wide range, precise temperature-programmed desorption (TPD) [12]. With a two-stage expansion cryostat and a heat switch operated with pressurizable bellows, we now reach stable 2.3 K at the sample, while still controlling rapid heating (to 1000 K for crystal cleaning) and cooling (to keep the sample clean). Temperature measurement and control via carefully calibrated thermocouples [10], electron bombardment, and a special regulator enabled controlled heating rates between 0.01 and 5 K/s. TPD spectra, for determination of both sticking and desorption rates, were acquired with a mass spectrometer in a “Feulner cap” [13] arrangement. During desorption, the cap covered the full solid angle seen by the surface; initially it was kept at room temperature (RT). When nonthermal desorption turned out to be appreciable, the cap temperature was made variable between 90 and 470 K. Pt(111) was chosen because its clean, low defect preparation, as well as rare gas adsorption on it, are well characterized [11]. The dosed helium gas was either at RT or 90 K. TPD spectra over 4 orders of magnitude in the rate were so reproducible that the rate could be calibrated. Both  $^4\text{He}$  and  $^3\text{He}$  mono- and submonolayers were investigated. Multilayers cannot form at 2.3 K and the low pressures used because of the weak He-He interaction.

After saturation of the surface with helium with both the environment seen by the surface and the He dosing gas at RT, a relatively small, unstructured desorption peak between 3.3 and 4.2 K was obtained. Below the peak, a further desorption signal was seen which slowly decreased during heating [Fig. 1(a)]. For  $^3\text{He}$ , this latter signal was distinctly larger, and the decrease faster. The initial decline proved not to be connected to the (increasing) *temperature*, but to the *time elapsed* (see below). Cooling the cap, i.e., the environment seen by the surface, to 90 K eliminated most of this prepeak signal, increased the total amount desorbed under the thermal peak by about 50%, and introduced structure similar to the

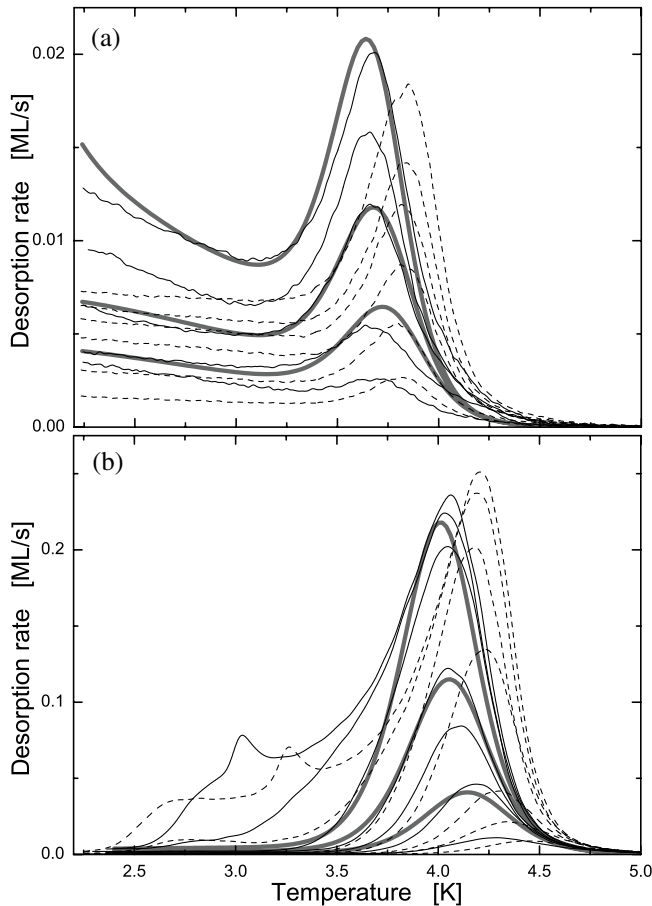


FIG. 1. (a) TPD spectra of  $^4\text{He}$  (dashed lines) and  $^3\text{He}$  (solid lines) layers produced by adsorption at gas and surround temperatures of 295 K. Maximum coverage 0.7 ML; heating rate 0.03 K/s. (b) layers up to 1 ML produced at gas and surround temperature of 90 K, 0.02 K/s. The appearance of compression peaks and the elimination of photodesorption are obvious. In each set, three theoretical curves for  $^3\text{He}$  are shown for initial coverages (top) 0.24, 0.41, 0.72, and (bottom) 0.12, 0.32, 0.57.

“compression peaks” well known from other rare gases [11,12,14], for both isotopes [Fig. 1(b)]. We therefore assume that we thus obtain a compressed, essentially saturated monolayer. The lower saturation coverage with both environment and gas at RT partly arose from collisional desorption: Energetic He gas atoms in the thermal distribution at RT knock off adsorbed atoms, lowering the maximum steady state coverage. This was corroborated by decreasing the He gas temperature, and by letting RT He impinge on other layers, e.g., neon on Pt(111). However, the slow desorption seen in the TPD runs below 3 K cannot be caused by this mechanism, as no He atoms impinge under TPD conditions. Varying the time between exposure of the surface and start of the heating procedure, as well as following the decline at constant temperature, showed that the *entire* coverage was susceptible to this slow desorption, and that its rate was proportional

to the coverage to good approximation (Fig. 2) yielding a first order desorption rate constant of  $\approx 0.01 \text{ s}^{-1}$  for  $^4\text{He}$ , higher by  $\times 1.5$  for  $^3\text{He}$ , for RT surroundings. Below 3.0 K, the onset of genuine thermal desorption, this rate was nearly independent of substrate temperature; only very careful tests showed a small gradual increase by less than 10% over the temperature increase from 2 to 3 K (see Fig. 2). We call this the photodesorption (PD) rate,  $R_{\text{ph}}$ .

Decreasing the environmental temperature seen by the surface by cooling the cap to 90 K decreased  $R_{\text{ph}}$  by a factor of about 4 for  $^3\text{He}$  and by 5–6 for  $^4\text{He}$ ; so it is barely apparent in Fig. 1(b). The dependence of the PD rate on the cap (i.e., radiation) temperature showed considerable scatter but had a roughly linear dependence and certainly not  $\sim T^4$  as expected if the rate were proportional to the energy density of blackbody radiation. A number of careful tests which cannot be detailed here [15] proved that sample heating definitely does not cause this desorption, and that normal thermal desorption (above 3 K) and this photoinduced effect are independent and additive.  $\text{H}_2$  and  $\text{D}_2$  monolayers, but not Ne, also showed this photoinduced desorption [16], as has also been reported before for hydrogen on Cu(510) [7].

We conclude that there are two independent, separable mechanisms of desorption in our TPD spectra: PD induced by far-infrared (FIR) photons coupling directly into the surface adlayer, and normal thermal desorption. For the spectra from (sub)monolayers produced and desorbed with 90 K gas and surroundings, the first contribution is small and the TPD spectra can be interpreted in the standard manner. Evaluation of the desorption parameters by various methods [12,17] (rising edge analysis, isosteric analysis, curve fitting) yielded a desorption

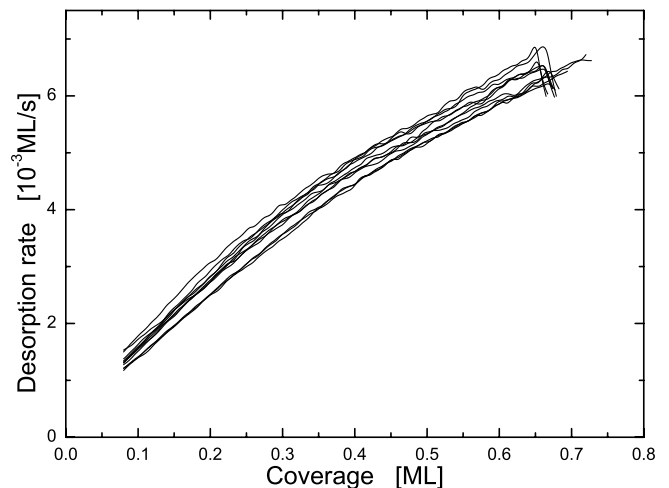


FIG. 2. Isothermal photodesorption in the range 2.3 (lowest curve) to 3 K (topmost curve), with RT surroundings, for  $^4\text{He}$ . Time runs from right to left. A slight deviation from first order kinetics is visible. A small but systematic rate increase with increasing temperature is seen.

energy of about 9 meV, and preexponentials rising from  $10^9 \text{ s}^{-1}$  at zero coverage to  $10^{11} \text{ s}^{-1}$  at 1/2 ML. In the compression range, the energy is about 20% smaller. For the spectra from layers produced and desorbed with gas and surroundings at RT, the contributions of thermal and photodesorption can be separated and analyzed individually. The single TPD peak around 4.2 K for  $^4\text{He}$  (4.0 K for  $^3\text{He}$ ) for coverages below about 0.7 of saturation (obtained as RT saturation, or for lower exposures at 90 K surroundings) is characteristic of a 2D gas with interactions; it moves to lower  $T$  with increasing coverage.

Sticking coefficients obtained via TPD peak integrals behaved with coverage as expected [12,18]: a very low value for the bare surface rising with coverage due to the better mass match of He colliding with adsorbed He; a broad maximum in the range of half coverage; and a gradual decline towards zero at saturation because of the filling of the monolayer. We thus get [15] the bell-shaped curve predicted for a monolayer without multilayer intermediates, seen previously [19,20] for the heavy rare gases on Pt(111). On the bare surface, we obtain  $S_0 \approx 0.02$  for 90 K gas and about a factor of 10 smaller at 300 K. Using the treatment of Ref. [18], these values can be extrapolated to 4 K, where we obtain  $S_0 \approx 0.03$ . This value and its coverage dependence are relevant for the calculation of thermal desorption, since sticking enters the preexponential through detailed balance.

The task of the theory is made easier by the independence of the two channels, thermal and photodesorption. PD is caused by the coupling of the electromagnetic field of the impinging thermal radiation into the dynamic dipole of the adsorbate. This is mediated in the dipole approximation by a Hamiltonian  $H_{\text{em}} = -\hbar(Q/m)\mathbf{A}(\mathbf{x}, t) \cdot (\partial/\partial\xi)$ . Here  $\mathbf{x}$  and  $\xi$  are center of mass and relative coordinates of the dipole, and  $m$  is its reduced mass. The effective charge  $Q$  is related to the dynamic dipole by  $Q = 2^{-1/2}\partial\mu_{\text{dyn}}/\partial z$  [8,9]. We can envisage two scenarios. (i) The dipole is due to the polarization of the He atom itself. Radiation will then excite internal vibrations of this polarization cloud and cause desorption by energy transfer to the center of mass motion [9]. RT blackbody radiation is not sufficient for that, and the small polarizability of He also makes this very inefficient. (ii) The dipole derives from the charge redistribution in the surface which the adsorbed helium induces and which changes when it moves; i.e., it mainly involves metal electrons. For this scenario, also considered elsewhere [6], we have used density functional theory for the estimation of polarizabilities, and of static and dynamic dipole moments.

The photodesorption rate constant is given by [8,9]

$$R_{\text{ph}} = \sum_{\mathbf{q}} \frac{2\pi}{\hbar} \sum_{\beta} \int d\mathbf{k} \Omega_{\mathbf{k}}^{-1} |\mathbf{M}_{\mathbf{q}0} \cdot \mathbf{U}_{\mathbf{k}\beta}(0)|^2 \times n_{\mathbf{k}\beta} \delta(E_{\mathbf{q}} - E_0 - \hbar\Omega_{\mathbf{k}}). \quad (1)$$

Here the sum over  $\mathbf{q}$  runs over the atomic continuum states reached from the ground state via a matrix element,

$$\mathbf{M}_{\mathbf{q}0} = i\hbar \frac{Q}{m} \sqrt{\frac{\hbar}{2\varepsilon_0}} \int d\mathbf{x} u_{\mathbf{q}}(\mathbf{x}) \frac{\partial}{\partial\mathbf{x}} u_0(\mathbf{x}). \quad (2)$$

Contributions from higher bound states in the helium surface potential are negligible [1].  $\mathbf{U}_{\mathbf{k}\beta}(0)$  is the field amplitude (of polarization  $\beta$  and wave vector  $\mathbf{k}$ ) at the position of the atom, and  $n_{\mathbf{k}\beta}$  is the Bose-Einstein occupation of photons at temperature  $T_r$ . As the simplest approximation, we take a Gaussian for the ground state wave function and plane waves for the continuum states.

For the depth of the surface potential, we take  $V_0 = 11 \text{ meV}$  and for the zero point energy  $\hbar\Omega/2 = 2 \text{ meV}$  from jellium calculations [21]; so  $E_0 = V_0 - \hbar\Omega/2$  equals the desorption energy. An effective charge [8,9]  $Q \approx 0.05\text{--}0.1e$  results from the density-functional theory calculations. For these parameters  $R_{\text{ph}}$  rises, for radiation temperatures  $T_r$  from 90 to 290 K, roughly linearly with  $T_r$  by a factor of 5–6, which is about the ratio of the Planck distributions at  $V_0$  for these two temperatures. This is the best evidence for a direct photoinduced process. We get  $R_{\text{ph}} \approx 0.006 \text{ s}^{-1}$  at 290 K, in good agreement with experiment. This corresponds to a quantum efficiency  $10^{-6}$  to  $10^{-7}$  desorbing He per incident photon.

The total rate of desorption is the sum of photodesorption and thermal desorption:

$$\left. \frac{d\theta}{dt} \right|_{\text{des}} = - \left[ R_{\text{ph}} + S(\theta, T) \frac{k_B T}{h} e^{\{V_0 - [\hbar(\Omega)/2]\}/k_B T} \right] \times e^{\mu(\theta, T)/k_B T}. \quad (3)$$

The latter is calculated with standard lattice gas techniques, for the low temperature regime,  $\hbar\Omega \gg k_B T$ , and for a system in which surface corrugation can be neglected [22].  $S(\theta, T)$  is the sticking coefficient (see above) and  $\mu(\theta, T)$  is the adsorbate chemical potential accounting also for the  $\theta$  and  $T$  dependences due to the lateral He-He interaction (we exclude the compression range here).

Our estimate of  $V_0$  fits the low coverage TPD traces for  $^3\text{He}$  at the high heating rate where PD is negligible, Fig. 1(b). The TPD peak shift to lower temperatures with increasing coverage is explained by the strong increase of sticking with coverage: The prefactor in (3) increases accordingly, shifting desorption to lower temperatures, Fig. 1(a). The lateral interaction is less important: We estimate an effective attraction between He atoms in a relaxed monolayer (corresponding to the single TPD peak) of  $-0.06 \text{ meV}$ , an order of magnitude smaller than the two-body potential minimum for the 3D gas and consistent with theoretical estimates for 2D He on various substrates [23]. The decrease from gas to surface is consistent with a dipolar He-He repulsion on the metal surface which, using the calculated dipole moment, is of the order of 1 meV. A critical temperature of about 0.5 K

results, below which a mobile adsorbate on a flat surface would undergo 2D condensation. With the parameters deduced for  $^3\text{He}$ , we calculate the TPD spectra for  $^4\text{He}$  by only changing  $\Omega$  by  $(4/3)^{1/2}$ , which shifts the peaks up by about 0.3 K and leads to good agreement also for the  $^4\text{He}$  curves (not included in Fig. 1 for clarity).

With these parameters for  $^3\text{He}$ , we can fit the initial desorption rates for the conditions of Fig. 1(a); we find  $R_{\text{ph}} = 0.013 \text{ s}^{-1}$ . No further parameter adjustments are required to obtain the remainder of these spectra. As to the isotope effect,  $R_{\text{ph}}$  varies similar to  $m^{-3/2}$  in agreement with experiment. The result is to decrease the PD rate for  $^4\text{He}$ , again without further adjustment. The initial desorption rate for the high heating rate data and 90 K environment, Fig. 1(b), is well fitted by reducing  $R_{\text{ph}}$  by a factor 4, consistent with our theoretical estimate. The agreement between theory and experiment is excellent in all aspects.

Comparing to the other literature reports on nonthermal desorption of weakly bound adsorbates, we note that all phonon-mediated mechanisms [5,24] would lead to a *reversed* isotope effect: The collisional coupling to phonons is *smaller* for a lighter adsorbate [18]. Such mechanisms should contribute strongly for insulators with their high bulk absorption in the FIR. On metals, on the other hand, absorption in the bulk is small, while the modification of the “soft” wave function tails on their surface by the adsorbate make the direct photon coupling to the latter strong. The fact that PD rates are smaller for hydrogen [7] indicates that the effect of the deeper adsorption well outweighs an expected increase in the dipole matrix elements. A quantitative evaluation is in progress.

In summary, in the first investigation of adsorption/desorption kinetics of  $^4\text{He}$  and  $^3\text{He}$  on a macroscopic single crystal surface, Pt(111), which we use to extract kinetic parameters, we have also found a quantum effect, photodesorption by far-infrared photons through direct coupling to the transition dipole induced in the surface by adsorbed helium. The proposed theory can recover the main properties of both the thermal and the photoinduced desorption; for the latter these are its approximate absolute magnitude, and its dependences on radiation temperature and on mass. As expected from earlier work [1,23], quantum effects are not significant in the main thermal desorption range, as shown by our reproduction of the desorption parameters and again their isotope effect.

We thank P. Feulner and W. Frieß for valuable discussions. The work in Munich was supported by the Deutsche Forschungsgemeinschaft through SFB 338/TP

C11, that at Dalhousie University by grants from the Office of Naval Research and by the Natural Sciences and Engineering Research Council of Canada. The cooperation of our groups was supported by the Alexander von Humboldt-Stiftung.

- 
- [1] H.J. Kreuzer and Z.W. Gortel, *Physisorption Kinetics* (Springer-Verlag, Berlin, 1986).
  - [2] L. Bruch, M.W. Cole, and E. Zaremba, *Physical Adsorption: Forces and Phenomena* (Oxford University Press, Oxford, 1997).
  - [3] M.W. Cole, D. R. Frankl, and D. L. Goodstein, *Rev. Mod. Phys.* **53**, 199 (1981).
  - [4] M. Weimer, R. M. Housley, and D. L. Goodstein, *Phys. Rev. B* **34**, 5199 (1987), and references therein.
  - [5] D. L. Goodstein *et al.*, *Phys. Rev. Lett.* **54**, 2034 (1985).
  - [6] K. A. Pearlstine and G. M. McClelland, *Surf. Sci.* **134**, 389 (1983).
  - [7] M. Hassel *et al.*, *Phys. Rev. Lett.* **80**, 2481 (1998).
  - [8] Z. W. Gortel *et al.*, *Phys. Rev. B* **27**, 5066 (1983).
  - [9] P. Piercy, Z. W. Gortel, and H. J. Kreuzer, in *Advances in Multi-Photon Processes and Spectroscopy*, edited by S. H. Lin (World Scientific, Singapore, 1987), Vol. 3, p. 105.
  - [10] H. Schlichting and D. Menzel, *Rev. Sci. Instrum.* **64**, 2013 (1993).
  - [11] W. Friess, H. Schlichting, and D. Menzel, *Phys. Rev. Lett.* **74**, 1147 (1995); W. Friess, Ph.D. thesis, TU München, 1995.
  - [12] H. Schlichting and D. Menzel, *Surf. Sci.* **272**, 27 (1992); H. Schlichting and D. Menzel, *Surf. Sci.* **285**, 209 (1993).
  - [13] P. Feulner and D. Menzel, *J. Vac. Sci. Technol.* **17**, 662 (1980).
  - [14] W. Widdra *et al.*, *Phys. Rev. B* **57**, 4111 (1998).
  - [15] T. Niedermayer *et al.* (to be published).
  - [16] T. Niedermayer, Ph.D. thesis, TU München, 2002.
  - [17] ASTEK software package by H. J. Kreuzer and S. H. Payne (Helix Science Applications, 618 Ketch Harbour Road, Portuguese Cove, Nova Scotia, Canada B3V 1K1).
  - [18] H. Schlichting *et al.*, *J. Chem. Phys.* **97**, 4453 (1992).
  - [19] P. Zeppenfeld *et al.*, *Surf. Sci. Lett.* **318**, L1187 (1994).
  - [20] H. J. Kreuzer, *Surf. Sci. Lett.* **344**, L1264 (1995).
  - [21] E. Zaremba and W. Kohn, *Phys. Rev. B* **15**, 1769 (1977).
  - [22] See, e.g., H. J. Kreuzer and S. H. Payne, in *Computational Methods in Surface and Colloid*, edited by M. Borowko (Marcel Dekker, New York, 2000).
  - [23] R. L. Siddon and M. Schick, *Phys. Rev. A* **9**, 907 (1974); A. D. Novaco and C. E. Campbell, *Phys. Rev. B* **11**, 2525 (1975); P. A. Whitlock, G. V. Chester, and M. H. Kalos, *Phys. Rev. B* **38**, 2418 (1988).
  - [24] P. M. Ferm *et al.*, *Phys. Rev. Lett.* **58**, 2602 (1987), and references therein.